Investigation of the stability in the plasma wakefield accelerator FLASHForward

DESY Summer Student Programme, 2021

Lara San Martín Suárez
Universitat Politècnica de Catalunya, Spain

Supervisor
Sarah Schröder

September 9, 2021

Abstract

Plasma wakefield acceleration is a promising avenue for future compact and affordable GeV-level linear accelerations, which potentially will enrich the field of high-energy physics. Nevertheless, this technique faces difficulties in terms of beam quality and stability. This work gathers the study of causes for the acceleration instability in the external injection scheme of beam-driven plasma wakefield acceleration at FLASHForward. In particular, the effect of bunch charge, bunch compression and bunch separation jitter on the energy spread was analysed. A first study was done using a simplified beam profile (longitudinally as well as transversely gaussian). Eventually a more realistic scenario was investigated and benchmarked to experimental results.

Contents

1 Introduction

High-energy particle accelerators have been key in the development of particle physics, the understanding of matter and the discovery of fundamental particles, and beyond that have a wealth of direct applications in science, medicine and industry. However, these applications are limited due to the immense size and costs of particle accelerators. If GeV-levels of energy are required, the size of the accelerator could increase from meters to several kilometers. The most powerful particle accelerator that has been built thus far is the Large Hadron Collider, a circular accelerator with 27 km of circumference, whose construction has relied on an international partnership in order to face the costs of its set-up, operation and maintenance.

In recent years, plasma wakefield acceleration [1] has been found to be a promising approach to making linear accelerators smaller in size and therefore more accessible to science and industry. The beam-driven plasma acceleration process consists of a first injection of an ultra-relativistic electron beam in the plasma – usually referred to as "driving bunch" – which loses its energy to creating a charge-density wake from the positive ions and electrons present. A second ultra-relativistic bunch – referred to as "trailing bunch" – is injected afterwards in the rare of the wake, leading to GeV-level acceleration requiring only few centimeters of propagation.

Ground-breaking results have been discovered during the past few years using this particular technique, which allows efficient acceleration at high gradients of energy gain per unit length [2, 3]. The FLASHForward facility [4] is positioned as an unique test-bed facility for stable and high-quality plasma wakefield acceleration worldwide as well as precision studies of this acceleration process [5]. However, there are still some issues that beam-driven plasma wakefield acceleration is facing nowadays — some of them being the difficulty of preserving the beam quality while being accelerated and the unwanted high values of energy spread.

One of the main causes of this instability in acceleration rely on a highly dependency to jitter in the creation of the plasma and the electron beam. The analysis presented in this report focuses on studying the effect that the different kinds of beam jitter have on the plasma wakefield created and final acceleration obtained. The aim is to present a bound on the most influential kinds of beam jitter and relate these to the final energy and energy spread. For that purpose, the study focuses in two different electron beams — one created virtually with all-gaussian profiles, which allows a first approach to the analysis of instabilities, and the other extracted from an experiment [6] conducted at the FLASHForward facility.

This work was carried out using the quasi-static Particle-In-Cell code HiPACE++ [7, 8], an open-source portable (GPU-capable) emulator for beam-driven plasma-wakefield acceleration. In order to select the HiPACE++ geometrical parameters – box size, longitudinal and transverse resolution and number of particles – a convergence test was performed (see Appendix A).

2 Gaussian beam

As a first approach to understanding the physics behind the jitter and setting up the required tools, a simplified mono-energetic beam, with both gaussian transverse and longitudinal profiles is assumed. This beam, whose parameters are listed in Table 1, will be denoted as "gaussian beam" henceforth.

Parameter	Value
Charge	1 nC
Energy	1 GeV
Length	180 fs rms
Normalised emittance	1 mm mrad
Beta function	10 mm
Transverse profile	gaussian
Longitudinal profile	gaussian

Table 1: **Beam parameters**. These parameters represent a typical beam delivered by the FLASH linac.

After the generation of a FLASH-like electron bunch, as it is typically extracted into the FLASHForward beam line, the next step is to also mimic the bunch-pair generation at FLASHForward [9]. For this purpose, the edges of the absorbing masks in the dispersive extraction section are imitated by means of an error function with a finite sigma, which takes into account the limited resolution of the longitudinal current-profile modification due to a finite slice energy spread of the bunch.

In order to optimize the acceleration process in terms of resulting beam energy and energy spread, different aspects have to be considered at the same time. On the one hand, the accelerated bunch should experience high negative fields in order to be accelerated as much as possible. On the other hand, in order to accelerate every particle of the injected bundle with the same gradient, the wakefield must be flattened along the extent of the injected bunch. Wakefield-flattening is achieved through loading a considerable amount of charge into the wakefield, the space charge of which then modifies the shape of the bubble and thus also the shape of the wakefield. Theoretically, the injected bunch for optimal beam loading would have finely adjustable trapezoidal current profile [10], which, however, is not available experimentally — a bi-sected Gauss is used as a good approximation to that. The critical parameters for flattening the wakefield are the plasma density, which changes the shape of the driven wakefield, the cut-out position as well as the cut-out width, which relates to the peak current and charge distribution among the two bunches and the longitudinal position of the injected beam in the wakefield respectively. These parameters were adjusted such that a sufficiently flattened wakefield was found.

Taking into account these variables, $3.15 \cdot 10^{16}$ cm^{-3} is found to be the optimal plasma density for acceleration. The cut-out width is fixed to absorb the 30% of the bunch charge with the cut-out position being displaced by $-7.5\,\mu$m in respect to the beam centre. In Fig. 1 the final driving and trailing bunches and the plasma blow-out bubble are depicted.

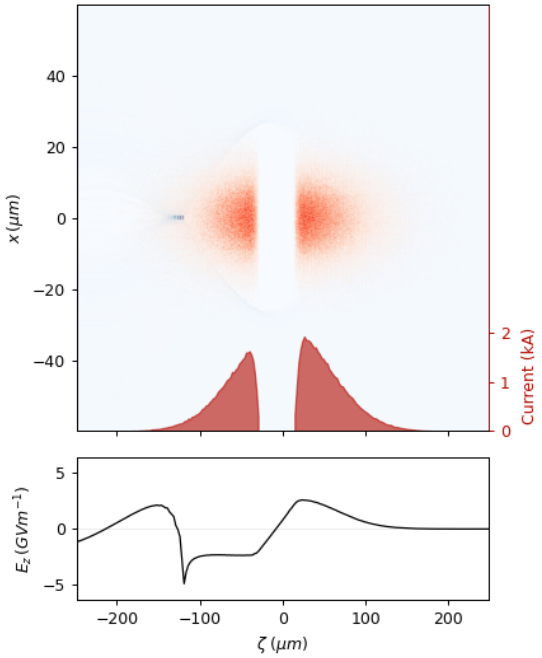

Figure 1: **Optimised beam–plasma interaction of the bisected Gauss beam**. Top: The drive bunch generates a strong blowout in the plasma (blue) in which a trailing bunch can be accelerated. The current profiles are optimised to flatten the wakefield along the extent of the trailing bunch (bottom). An accelerating field on the order of GVm^{-1}-level is achieved

In order to match the experimental configuration at FLASHForward, the beams are propagated up to 50 mm. The main objective is to study the final energy gain and energy spread in the trailing bunch – in Fig. 2 the evolution of the mean energy and energy spread is shown.

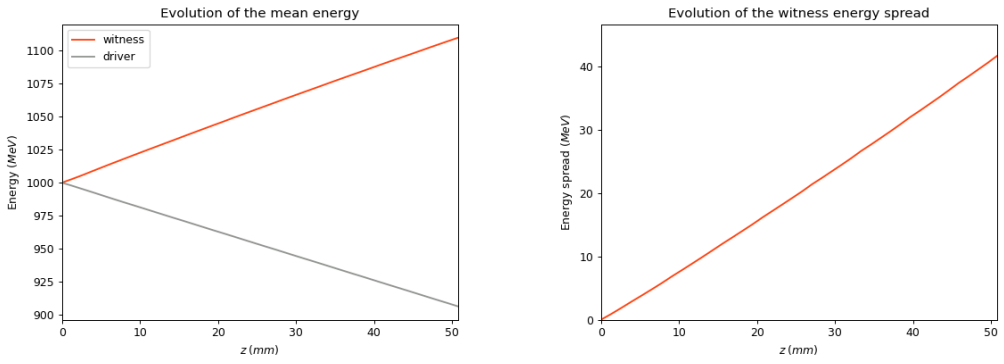

Figure 2: **Evolution of the mean energy (left) and the imposed energy spread (right) during beam–plasma interaction**. Left: The trailing bunch (red) experiences an 11% energy gain—a final mean energy of 1110 MeV is achieved. Meanwhile, the driving bunch loses 9% of its energy. Right: Owing to the non-perfect wakefield flattening, an energy spread of 42 MeV is imprinted on the trailing bunch.

Due to the positioning of the trailing bunch tail, the difference in energy gradients throughout the bunch will lead to a leak of particles. For that reason, only the particles with a divergence within the first step limits are taken into account in our evolution analysis.

2.1 Beam jitter analysis

Owing to the small structure of the "plasma acclerator cavity" and the prevalence of strong GVm^{-1}-level longitudinally accelerating and transversely focusing fields, the resulting stability of a plasma accelerator depends crucially on the stability of those plasma as well as beam parameters that affect the field strength or include spatial dependencies. For the purpose of analysing these instabilities in the acceleration process, a study is presented of different sources of jitter for the electron beam. Based on the experience gathered in previous experiments, the study was focused in the following parameters:

- **Original bunch charge**. This jitter mainly comes from instabilities of the photo-injector laser in the FLASH linac.
- **Bunch compression**. This jitter is mainly caused by an orbit jitter in the compression sections of the FLASH linac.
- **Bunch separation position**. This jitter results in a jitter in peak current of the driving and trailing bunch as well as a jitter in charge distribution among the two bunches. It is caused by an orbit jitter of the original FLASH electron bunch at the position of the collimators, which eventually bi-sect the bunch into the bunch pair needed for external injection plasma wakefield acceleration.

In order to represent the experimental condition, similar jitter amplitudes as the ones found in experiments were implemented. The main objective throughout this stability study is the final energy gain and the imposed energy spread on the trailing bunch.

Charge jitter

An analysis is presented of the change in longitudinal wakefield shape for 11 different charge values. These 11 charge values were randomly chosen from a normal distribution with a mean value of 100 pC and a 5 pC standard deviation.

The resulting current profile error band is shown in Fig. 3. The change in the trailing and driving bunches' current provoked by the change in total charge has an effect in the wakefield amplitude as well as the beam loading effect, such that the highest field amplitudes in absolute value correspond to the highest charge value and as the smallest field amplitudes correspond to the lowest one. This change in the field is depicted in Fig. 4. By that it is shown that the wakefield strength is thus limited by the maximum and minimum values in charge.

Other characteristic values, as mean energy, energy spread or transverse beam size, remain constant.

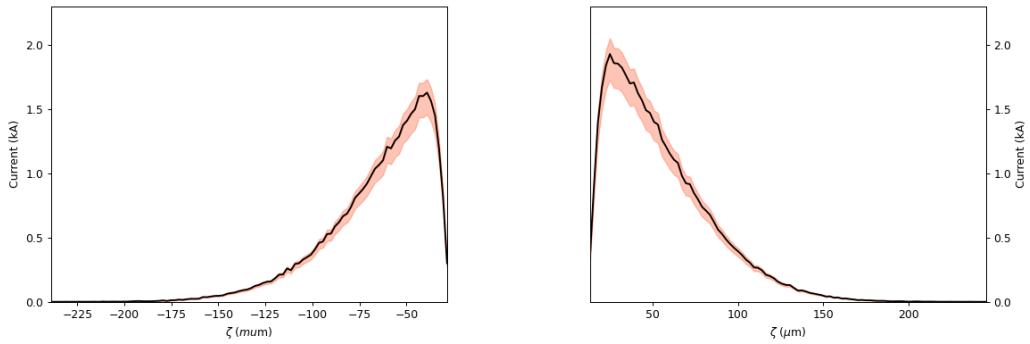

Figure 3: **Effect of the charge jitter on the current profile.** Current error bars for the trailing (left) and driving (right) bunches for the minimum and maximum beam charge values, which correspond to -10% and +6% jitter respectively.

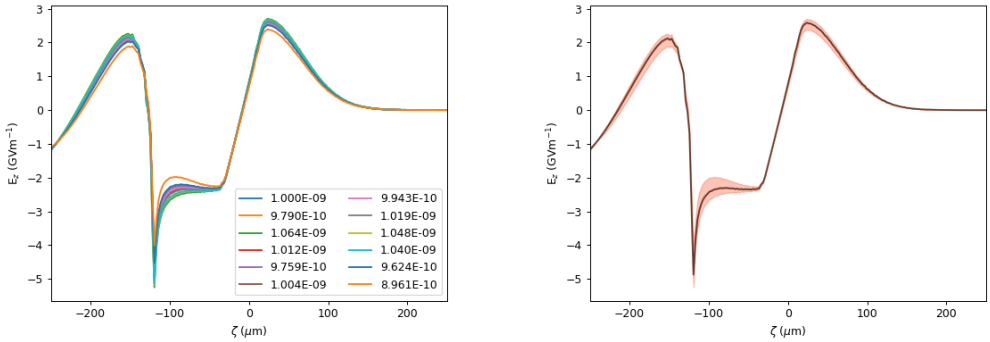

Figure 4: **Effect of the charge jitter on the wakefield.** The left plot shows the wakefield lineout for all the different randomly sampled beam charge values. The inner and outer orange lines correspond to the maximum and minimum respectively. The right plot shows the same wakefield with just the error limited by the minimum and maximum beam charge values, which correspond to -10% and +6% jitter respectively.

Compression jitter

To study the beam compression jitter, the standard deviation of the longitudinal gaussian profile is extracted randomly from a normal distribution with a mean value of 54 µm and 5.4 µm standard deviation. The analysis gathers 11 randomly chosen beam length values.

The jitter in the compression of the beam leads to a change in steepness of the edges in the trailing bunch tail and driving bunch head, being much more influential in the latter due to the unbalanced cut-out, as shown in Fig. 5. Because of this, the wakefield strength is more affected than with the charge jitter, as the growth in charge for the driving and trailing bunches is not equal anymore. It is the strongest for the compressed beams, with increased amplitude and a strong deviation from a wakefield-flattened operation point, as can be seen in Fig. 6.

The mean energy remains constant. However, the energy spread and transverse beam size present variations of the order of $10^{-2} - 10^{-3}$ of its original value.

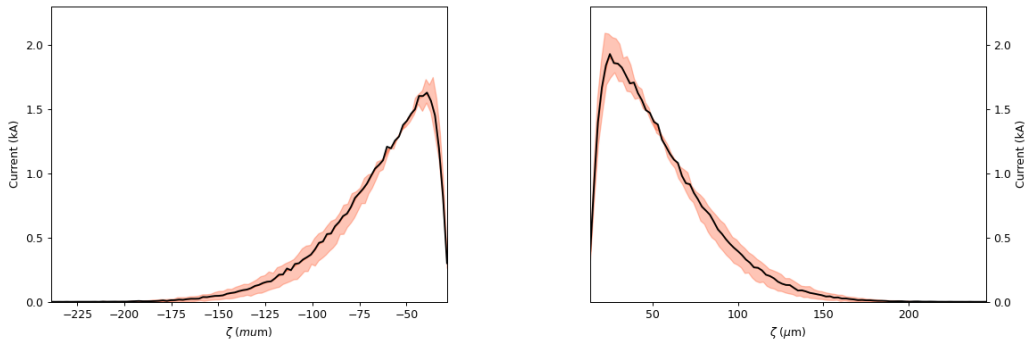

Figure 5: **Effect of the compression jitter on the current profile.** Current error bars for the trailing (left) and driving (right) bunches for the minimum and maximum beam length values, which correspond to -1% and +1% jitter respectively.

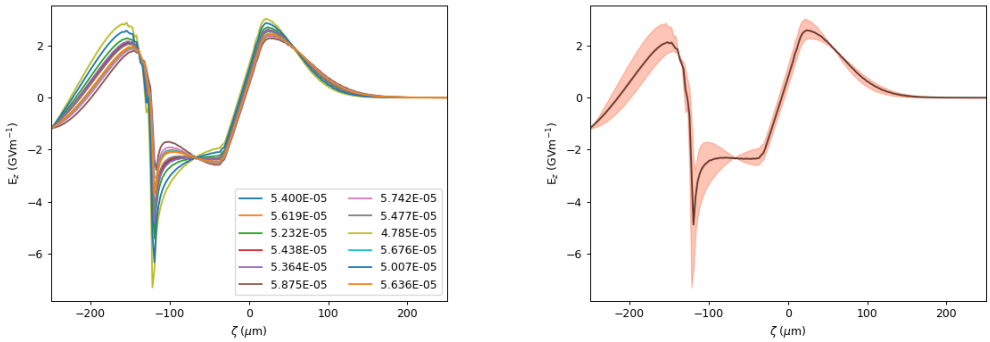

Figure 6: **Effect of the compression jitter on the longitudinal wakefield.** The left plot shows the on-axis wakefield lineout for all the different randomly generated compression settings. The inner and outer orange lines correspond to the maximum and minimum respectively. The right plot shows the same wakefield with just the error limited by the minimum and maximum beam length values, which correspond to a -1% and +1% deviation in compression respectively.

Separation jitter

A variation in cut-out position of 5%, 10% and 15% with respect to the total cut-out width was studied. A displacement to the positive z-direction will be referred using +5%, +10%, +15%, i.e. a gradual gain in bunch charge of the trailing bunch, and a displacement to the negative z-direction using -5%, -10%, -15%, i.e. gradual gain in bunch charge of the driving bunch.

In Fig. 7 the resulting wakefield created by the gaussian beam with the different cut-out position jitters is shown. The upper bound shown to the original field would correspond to +15% – +5% displacement jitter (top to bottom) and the lower bound to -15% – -5% displacement jitter (bottom to top). These jittered beams are propagated for 50 mm in order to study their effect on the final acceleration of the trailing bunch. Fig. 8 shows the corresponding bounds on the energy evolution plots.

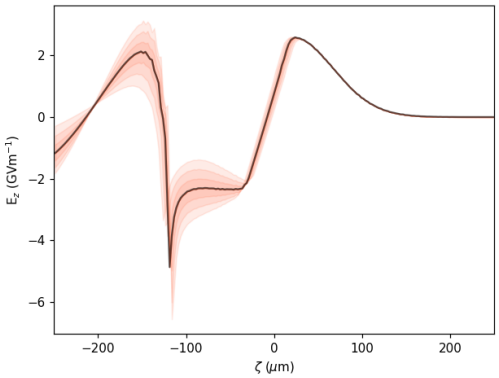

Figure 7: **Effect of the cut-out position jitter on the longitudinal wakefield.** While the amplitude of the driven wakefield stays pretty much constant as the head of the drive bunch was not modified, the wakefield experienced by the trailing bunch is significantly changed and the optimal flattening of it not maintained.

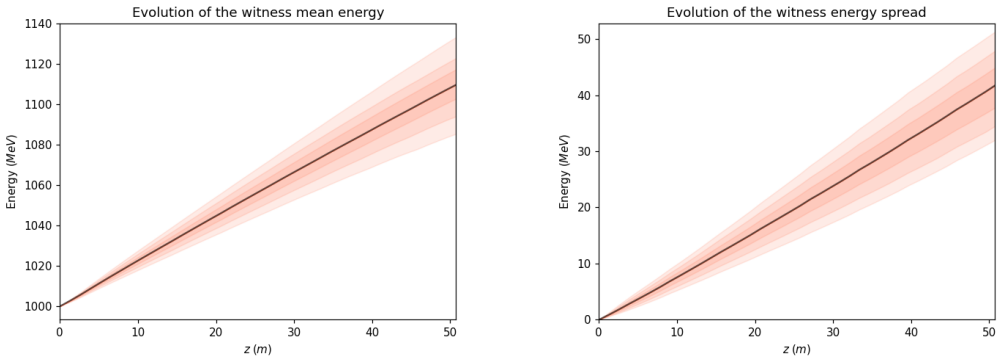

Figure 8: **Effect of the cut-out position jitter on the resulting mean energy and energy spread of the accelerated bunch.** Trailing bunch mean energy (left) and energy spread (right) evolution for the different jittered cases. The upper bound corresponds to -15% – -5% position jitter (top to bottom) and the lower bound to +15% – +5% position jitter (bottom to top).

The cut-out position jitter is found to have a large impact on the trailing bunch energy values. For the largest jitter investigated in this study (±15%), a deviation of 23% in both the gained energy and energy spread was found. For the lowest jitter presented, the deviation is 7% for the gained energy and 9% for the energy spread. The results of the other jitter values can be found in Table 2. A needed stability beyond these values would require a stability of the cut-out position better than 5% of the total cut-out width.

Jitter value	Mean energy gain	Energy spread
± 15%	± 22.2%	± 23.3%
± 10%	± 14.2%	± 17.3%
± 5%	± 7.0%	± 9.5%

Table 2: **Deviation in the trailing bunch mean energy and energy spread for the cut-out position jitter**.

2.2 First conclusions

Based on the jitter studies discussed above, it was found that for each parameter (charge, compression and separation position) it is sufficient to process the maximum and minimum error values, which reduces the amount of simulations needed. Furthermore, it was found that an instability in bunch compression and bunch-separation position have a stronger effect on the wakefield shape than the charge jitter.

A crucial difference between these types of jitter lays on the fact that a charge instability changes the charge as well as the peak current of both, the driving and trailing bunches, simultaneously in the same direction, i.e. if the driving bunch gains more charge the trailing bunch also does. Thus basically only the absolute amplitude of the wakefield is changed throughout all phases (with additional minor changes in the optimal beamloading condition). A jitter in the cut-out position, however, changes the peak current and bunch charges vice versa, i.e. a higher charge / higher peak current in the drive bunch will ultimately mean that the trailing bunch has a a lower charge / lower peak current. This leads to a strong deviation from the optimal beamloading condition and thus a more significant spread in mean energy as well as energy standard deviation.

A jitter in the compression of the beam while maintaining a constant charge results in a change in steepness of the edges in the driving bunch head and trailing bunch tail. Because the cut-out of the gaussian beam is displaced from the middle by $-7.5\,\mu\text{m}$, the compression jitter has more effect on the driving bunch peak current than on the trailing bunch. That results in a deviation from the optimal beamloading operation point. The strength of the wakefield ultimately depends on the peak current of the drive bunch, which is then loaded with a trailing bunch whose peak current has increased with a smaller rate.

3 Experimental beam

Based on the understanding gained through the detailed study discussed above using a gaussian-profiled electron bunch, eventually a more realistic scenario is investigated in the following. More specific, the main causes of the remaining instabilities found in the publication [6] are investigated, with the primary objectives being the instability in mean energy and energy spread (Fig. 9).

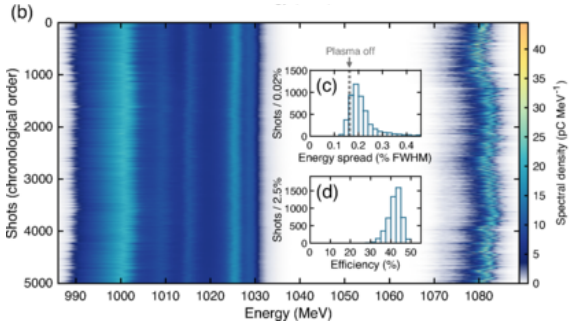

Figure 9: **State-of-the-art stability at the FLASHForward facility**. A high-statistics data set of 5000 consecutive shots of an optimally beamloaded acceleration working point illustrates the newly established stability in the field of beam-driven plasma wakefield acceleration. The mean energy spread in the data set is stable within 3% rms. The energy spread was preserved in about 6% of the shots, meanwhile the others have a relative increase in energy spread of about 30% developed in a 50 mm plasma channel. This instability can be understood as a result of jitter in beam as well as plasma parameters. (**Source**: C.A. Lindstrøm et al., Phys. Rev. Lett. **126**, 014801 (2021) [6])

For that purpose, the beam profile is extracted via graph digitisation, and the main characteristics of the beam can be found throughout the original paper.

To perform the cut-out of the beams, the information regarding the total driving and trailing bunch charges was implemented, and error functions with finite sigma were used to mimic the original cutting. Because not all of the data was used (e.g. the longitudinally resolved bunch parameters, slice energy spread, ...), a steeper cutting for the trailing bunch head was needed to achieve a similar amplitude of the wakefield and a proper flattening of the field. In Fig. 10 the comparison between the original profile and ours is shown. The final trailing and driving bunch charges were found to be of 120 pC and 490 pC respectively.

The beam is propagated 50 mm, the same propagation length used in [6], and the evolution of the mean energy and energy spread is shown in Fig 11. As with the gaussian beam, only the particles whose divergence is within the first step values were taken into account.

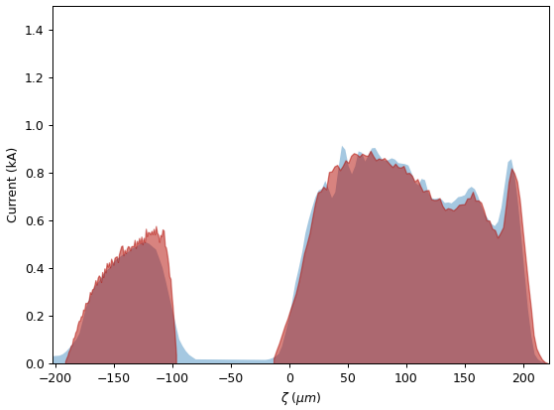

Figure 10: **Modeling the bunch separation of the experimental beam**. Error functions with finite sigma are used to model the resulting current profile of the drive and trailing bunch based on the original current profile of the uncollimated bunch. A sufficient agreement of the measured (blue) and the modeled current profile (red) is found.

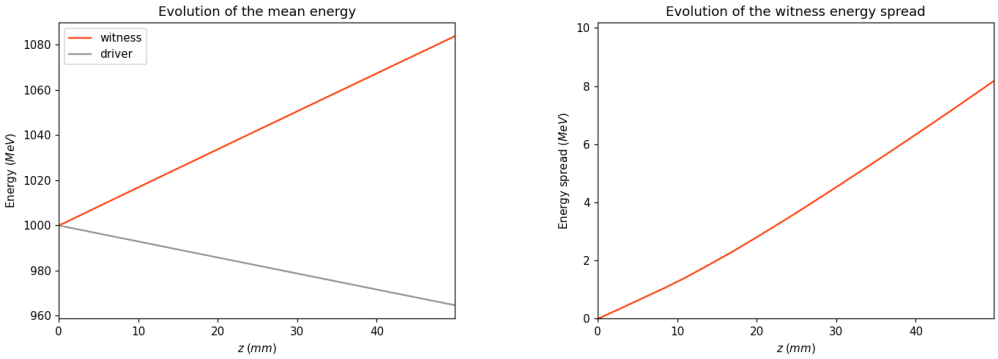

Figure 11: **Evolution of the mean energy (left) and the imposed energy spread (right) during beam-plasma interaction**. Left: The trailing bunch experiences an 8.4% energy gain—a final mean energy of 1084 MeV is achieved. Meanwhile, the driving bunch loses 3.5% of its energy. Right: An energy spread of 8.18 MeV is imprinted on the trailing bunch.

3.1 Modeling the bunch separation jitter

In order to mimic the 1.2% charge jitter after the bunch separation found in the experiment, a virtual separation position jitter on the previously modeled current profile is performed, which allows an extraction of the therewith resulting total charge. The relationship between the position of the cut-out and the total bunches' charge results in being close to linear, as is shown in Fig. 12. According to this result, a 1.2% charge jitter would correspond to a ∼5.3% cut-out position jitter with respect to the cut-out width. This actual beam-to-collimator displacement is assumed to be symmetric.

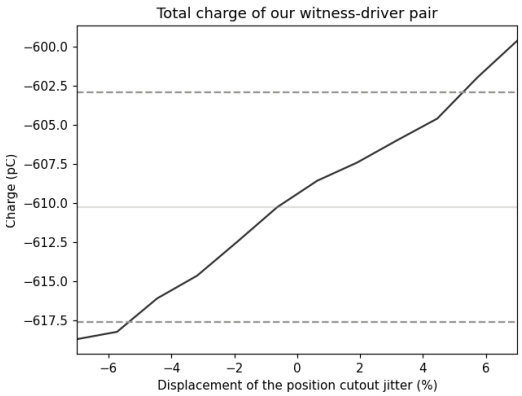

Figure 12: **Determination of the cut-out position jitter that relates to the experimental charge jitter downstream bunch-pair generation**. The originally to the sub-percent-level stable total charge of the bunch pair (gray) developes a remarkable 1.2% charge jitter (dashed) after bunch separation via collimation in a dispersive section. This bunch charge jitter can be understood as a beam orbit jitter at the location of the collimators and relates to a 5.3% displacement of the cut-out position as a fraction of the cut-out width.

3.2 Beam jitter analysis

Separation jitter

In Fig. 13 the evolution of the mean energy and energy spread of both beams are presented for the ±5.3% cut-out position jitter cases. The upper bound would correspond to the +5.3% displacement case and the lower bound would correspond to the -5.3% displacement case. The error produced in the trailing bunch mean energy is negligible – about 3% in gained energy. However, the error in the energy spread is of 16.75% and 17.5% for the upper and lower bound respectively.

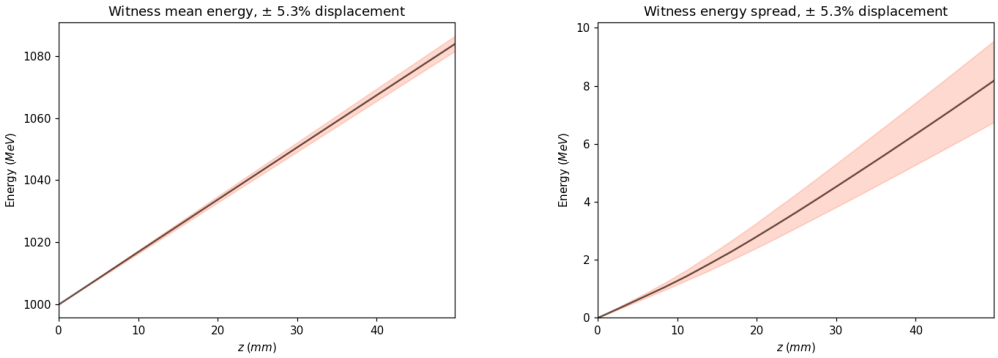

Figure 13: **Effect of the cut-out position jitter for a ±5.3% displacement on the resulting mean energy and energy spread of the accelerated bunch.** The trailing bunch mean energy (left) and energy spread (right) evolution for the +5.3% displacement case (upper bound) and -5.3% displacement case (lower bound) is shown.

In order to provide a bound for the energy deviation, a further analysis of the ±4%, ±3%, ±2% and ±1% displacement cases is presented.

In Fig. 14 the evolution of the trailing bunch energy spread is shown. The upper bounds would correspond to the -5.3% – -1% displacement cases (top to bottom), whereas the lower bounds would correspond to +5.3% – +1% (bottom to top).

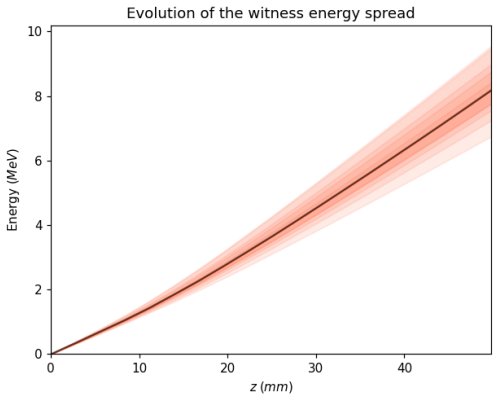

Figure 14: **Effect of the cut-out position jitter for ±5.3% – ±1% displacement on the resulting energy spread of the accelerated bunch**. Comparison of the trailing bunch energy spread evolution between the original bunch (black line) and the ±5.3% – ±1% position cut-out displacement.

For each jitter in the cut-out position there is a bound in the variation in the trailing bunch energy. In this scenario, the energy spread deviation was of 17% for the largest jitter (±5.3%). For the lower jitter presented, the deviation is of 5% — further results can be found in Table 3. If a energy deviation lower than 5% is needed, the position of the cut-out between the trailing and driving bunches would require a stability better than 1% of the total cut-out width.

Jitter value	Energy spread
± 5.3%	± 17.5%
± 4%	± 15.8%
± 3%	± 9.9%
± 2%	± 7.0%
± 1%	± 5.1%

Table 3: **Deviation in the trailing bunch mean energy and energy spread for the cut-out position jitter**.

Compression jitter

To study the beam compression jitter an error in the uncollimated beam length of ±1%, ±3% and ±5% is presented, while maintaining the overall charge, position and width of the cut-out. In Fig. 15 the trailing bunch energy evolution plots are shown. The upper bound corresponds to +5% – +1% compression jitter (top to bottom) and the lower bound to -5% – -1% compression jitter (bottom to top).

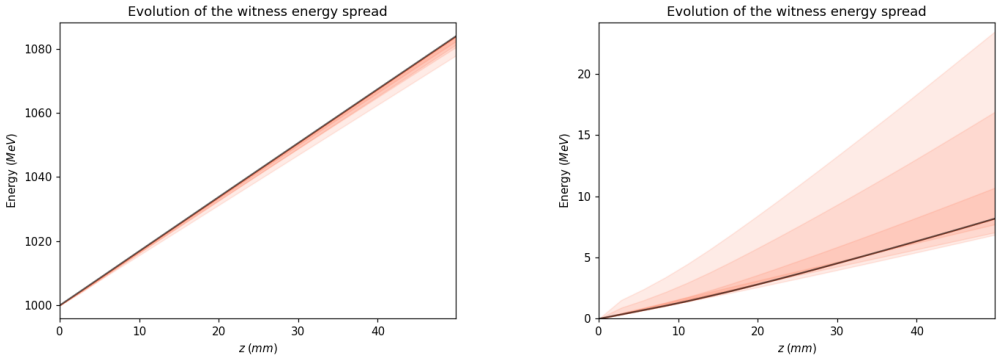

Figure 15: **Effect of the compression jitter on the resulting mean energy and energy spread of the accelerated bunch.** The trailing bunch mean energy (left) hardly experiences variation. However, the trailing bunch energy spread (right) experiences a 200% increment for the greatest beam length jitter (±5%). The upper bound corresponds to +5% – +1% compression jitter (top to bottom) and the lower bound to -5% – -1% compression jitter (bottom to top).

The deviation in energy spread is much higher in our compression beam study than in the cut-out positioning one. In Table 4 the resulting energy deviation for the different compression jitter values can be found.

Jitter value	Energy spread
± 5%	± 186.8%
± 3%	± 106.6%
± 1%	± 30.7%

Table 4: **Deviation in the trailing bunch mean energy and energy spread for the compression jitter**.

3.3 Conclusions

In this study, both the beam position cut-out and compression jitter have been found to be highly influential sources of energy spread deviation for this experimental beam.

There is an intention of recreating the same wakefield amplitude and flattening as in [6]. However, there are some left-out tasks that one could do to improve the similarity between this scenario and the experimental one, which would be:

- Incorporating the tail-to-head data: emmitance and energy spread. In our case, the experimental beam has an uniform emittance of 4 mm mrad. In order to improve the result, a 1-20 mm mrad emittance (tail and head respectively) should be implemented.

- Adjusting the new beam profile to better fit the original current profile, while maintaining the trailing and driving bunch charge and optimising the wakefield flattening.

4 Summary

In the scope of this project, the main causes of instability in a beam-driven plasma wakefield accelerator were investigated. Based on the experience from previous experiments, the main focus was on instabilities resulting from the jitter in beam parameters. More specific, a jitter in charge, which experimentally originates already in the bunch generation via photoelectric effect, a jitter in bunch compression, which is realised in magnetic chicanes, and a jitter in bunch separation, which is realised by the use of collimators in a dispersive section to separate a chirped electron bunch into two.

The compression and cut-out position were found to be the parameters of most importance. Moreover, a bound on these parameters was given for controlling the error in energy spread and keeping it to a minimum. Lastly, further optimisation that can be done to the electron beam was indicated to better match the experimental data.

An important remark would be that there are many other jitter values to take into account, such as transverse tilt, incoming angle or jitter in plasma parameters. However, this report focused on the three kind of beam jitter mentioned, based on the experience from previous experiments.

Acknowledgements

I want to thank the DESY Summer Student Programme organization for handing me this opportunity. I also want to thank my supervisor, Sarah Schröder, for all of her dedication and constant guidance on the project. She has helped me not only to get introduced to plasma wakefield acceleration, but has also motivated me deeply and was always available to answer all of my questions. I would also want to thank Severin for helping me to get started the very first weeks and solving all of my coding-related questions. Lastly, I want to thank all of the FLASHForward group for letting me be a part of their weekly meetings and for those 1-on-1 talks organised by Sarah where I could get to know the team, the different research conducted at FLASHForward and gained a sense of fellowship even by working remotely.

References

[1] T. Tajima and J. M. Dawson, Laser electron accelerator, Phys. Rev. Lett. **43**, 267 (1979)

[2] I. Blumenfeld, *et al.*, Energy doubling of 42 GeV electrons in a metre-scale plasma wakefield accelerator, Nature **445**, 741–744 (2007).

[3] M. Litos, *et al.*, High-efficiency acceleration of an electron beam in a plasma wakefield accelerator, Nature **515**, 92–95 (2014).

[4] R. D'Arcy, *et al.*, FLASHForward: plasma wakefield accelerator science for high-average-power applications, Phil. Trans. R. Soc. A. **377** 20180392, (2019)

[5] S. Schröder, *et al.*, High-resolution sampling of beam-driven plasma wakefields, Nat. Commun. **11**, 5984 (2020)

[6] C. A. Lindstrøm, *et al.*, Energy-Spread Preservation and High Efficiency in a Plasma-Wakefield Accelerator, Phys. Rev. Lett. **126**, 014801 (2021)

[7] T. Mehrling, *et al.*, HiPACE: a quasi-static particle-in-cell code, Plasma Phys. Control. Fusion **56** 084012 (2014)

[8] S. Diederichs, *et al.* (to be published)

[9] S. Schröder, *et al.*, Tunable and precise two-bunch generation at FLASHForward, J. Phys.: Conf. Ser. **1596** 012002 (2020)

[10] M. Tzoufras, *et al.*, Beam Loading in the Nonlinear Regime of Plasma-Based Acceleration, Phys. Rev. Lett. **101**, 145002 (2008)

A Convergence test

A.1 Gaussian beam

The following pictures show the wakefield for the different geometrical parameters: box size, number of particles, transversal and longitudinal resolution.

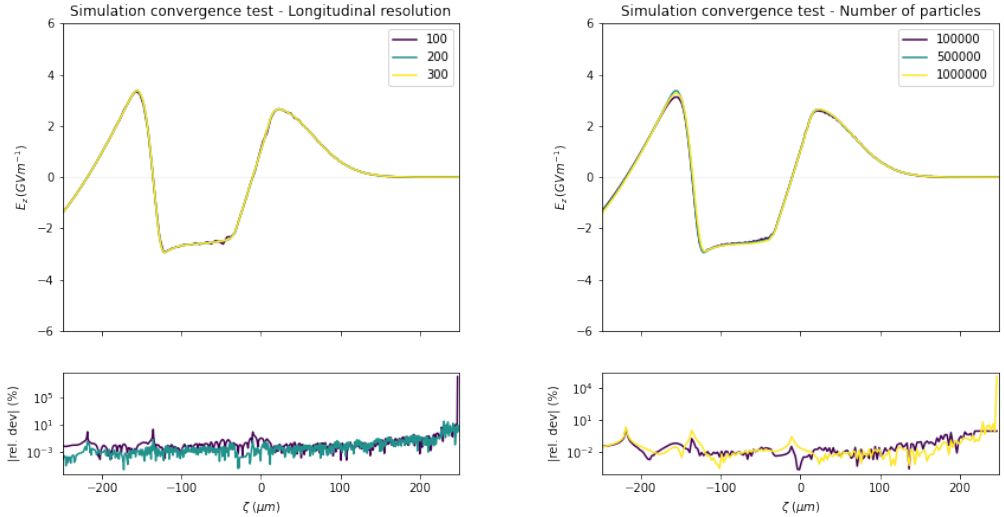

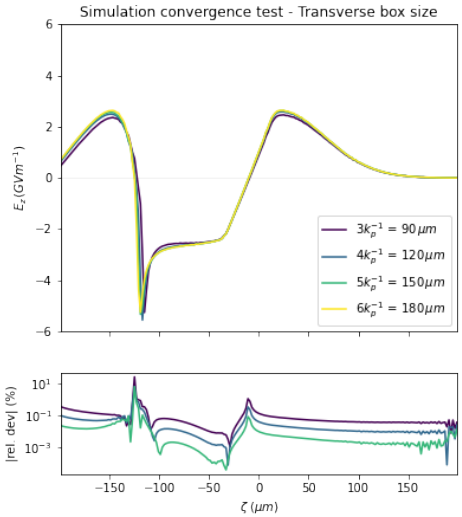

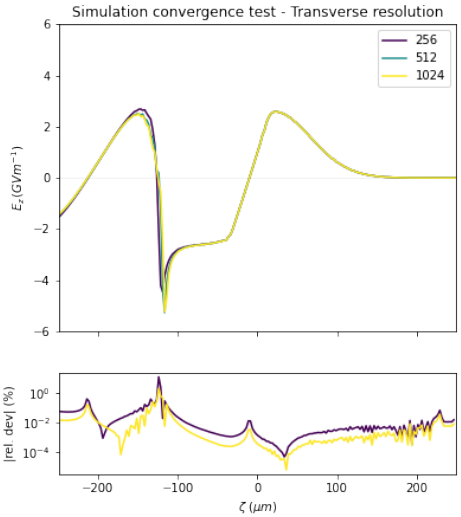

According to these images, the following parameters were set in our final simulations:

Parameter	Value
Box limits	120 µm
Number of particles	5e5 particles
Longitudinal resolution	200 grid points
Transverse resolution	512 grid points

Table 5: Graussian beam geometrical parameters.

A.2 Experimental beam

The following pictures show the wakefield for the different geometrical parameters: box size, number of particles, transversal and longitudinal resolution.

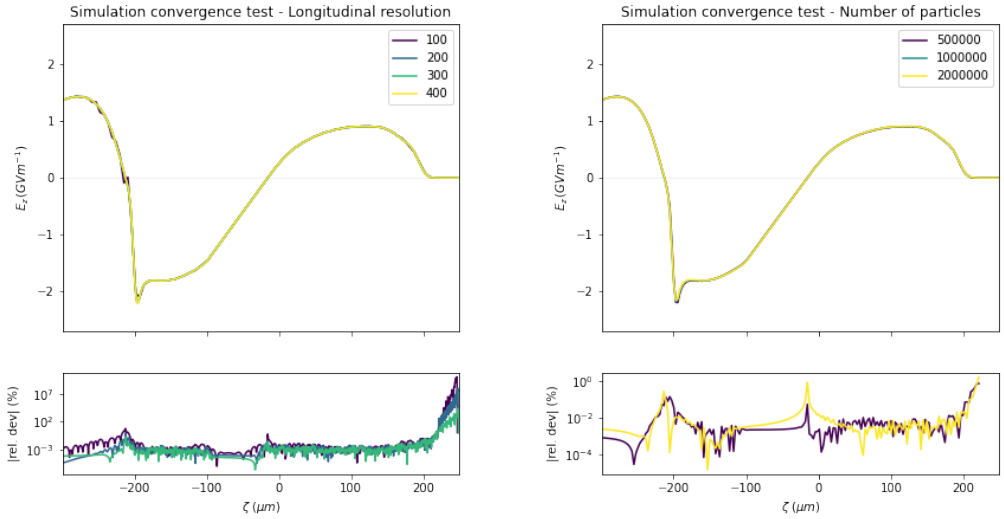

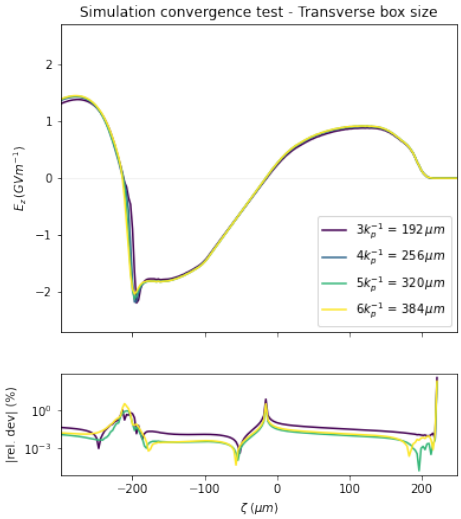

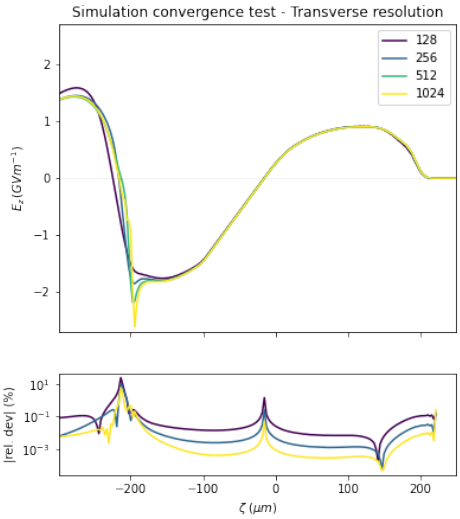

According to these images, the following parameters were set in our final simulations:

Parameter	Value
Box limits	256 µm
Number of particles	10e5 particles
Longitudinal resolution	200 grid points
Transverse resolution	512 grid points

Table 6: Experimental beam geometrical parameters.